Contribution 7

Long-lived signatures of conversion-driven freeze-out

B. Fuks, J. Heisig, A. Lessa, J. M. No, S. Sekmen, D. Sengupta, J. Zurita

Abstract
We consider a dark matter model where the relic density is set by conversion-driven feeze-out. This mechanism predicts long-lived particles at the LHC requiring small couplings and a relatively small mass splitting in the dark sector. As such it falls somewhat in between the typical targets of currently performed long-lived particle searches either considering extreme mass compressions or very small couplings, but lack their combinations. We study various search strategies covering the whole range of possible decay lengths $\mathcal{O}(1\,\text{mm} - 1\,\text{m})$, pointing out blind spots in the experimental search programme and estimating the corresponding potential for improvement.

1 Introduction

The existence of dark matter (DM) is one of the prime motivations for physics beyond the standard model (SM) and hence its detection consists in an important scientific goal of the LHC experiments. While the weakly interacting massive particle (WIMP) paradigm has mainly guided our DM search strategies in the past, other possibilities exist and have now come into focus. In this work we compare various search strategies for DM models containing long-lived particles with decay length $\mathcal{O}(1\,\text{mm} - 1\,\text{m})$, and small mass splittings $\mathcal{O}(10)$ GeV, as predicted by conversion-driven freeze-out [74, 75, 139]. As a benchmark model we take the one studied in [74] supplementing the SM by a Majorana fermion DM candidate and a scalar bottom partner, both odd under a new Z_2 symmetry under which all SM particles are even.

This example is interesting as it reveals blind spots in the performed LHC analyses targeted to other benchmark scenarios, where the long lifetime is typically considered to arise either from an extreme mass compression (long-lived chargino scenario) or a very small (effective) coupling (*e.g.* split supersymmetry or gravitino scenarios). However, the case in-between, as it occurs here, is often not explicitly considered.

We study various different searches aiming at covering as much of the model parameter space as possible. For very small decay lengths, common DM searches requiring missing energy plus jets can be applied [140, 141]. These searches typically assume direct DM production, or its production via the prompt decays of a parent particle. Depending on the inclusiveness of the search, the latter could also be sensitive to intermediate decay lengths. However, as the corresponding SM backgrounds are sizeable, missing energy searches are typically outperformed by dedicated searches towards large decay lengths.

For very large decay lengths $\gtrsim 1\,\text{m}$, searches for heavy stable charged particles (in this case R-hadrons) [138, 142–144] can be applied and provide great prospects while being extremely inclusive. However, the sensitivity drops quickly for smaller decay length due to the exponentially suppressed number of R-hadrons passing through the whole detector. Therefore, intermediate lifetimes can only be sensitively searched for when exploiting the displaced decay of the parent particle. In this respect we consider searches for disappearing tracks [145], displaced jets [146] and delayed jets [147]. However, these searches are less inclusive than the two cases mentioned above. Furthermore, displaced and delayed jets searches are not targeted to small mass splittings, and hence soft visible decays of the long-lived parent particle.

2 The dark matter model

We extend the SM by a singlet Majorana fermion DM candidate χ and a colored scalar bottom partner $\tilde{b}$ both transforming odd under a new Z_2 symmetry (while SM particles are even). The new physics interactions are described by

$$\mathcal{L}_{\text{int}} \subset D_\mu \tilde{b}^\dagger D^\mu \tilde{b} - \left(\lambda_\chi \tilde{b} \bar{b} \frac{1-\gamma_5}{2} \chi + \text{h.c.} \right), \tag{1}$$

where b is the b-quark field, D_μ the covariant derivative and λ_χ the DM coupling. The model resembles a supersymmetric simplified model with a bino-like neutralino and a right-handed sbottom, except for the coupling λ_χ, being considered a free parameter here. Within the model, conversion-driven freeze-out allows one to explain the measured relic density for small couplings, $\lambda_\chi = \mathcal{O}(10^{-7} - 10^{-6})$ and relatively small mass splittings, $\Delta m_{\chi \tilde{b}} = m_{\tilde{b}} - m_\chi \lesssim 35\,\text{GeV}$ [74]. The respective parameter space resides below the thick black curve in Fig. 1. The thin green and grey dotted curves denote contours of constant coupling and decay length, respectively, predicting the measured relic density, $\Omega h^2 \simeq 0.12$ [77]. A qualitatively similar phenomenology is obtained for a model with a top partner [78] or a leptonic partner [148].

3 Search strategies

As the bottom partner $\tilde{b}$ is strongly interacting, its pair-production cross section at the LHC is large. In the regime of non-prompt decays considered here, it hadronizes and forms R-hadron bound states before decaying into a b-quark and DM. The corresponding process is sketched in Fig. 2. In the following we study and discuss various search strategies in the context of this signature.

3.1 Missing energy searches

Among the most inclusive search strategies are missing energy searches. In Ref. [74], the results of an early Run 2 ATLAS monojet search for new physics in 3.2 fb^{-1} of LHC data [140] have been reinterpreted. The red curve in Fig. 1 shows the boundary of the correspoding 95% confidence level (CL) exclusion (the red shaded area being excluded), as taken from [74]. In the experimental analysis, a signal is selected by requiring events to feature a large amount of missing transverse energy ($E_T^{\text{miss}} > 250$ GeV) and a hard central leading jet with a transverse momentum p_T larger than 250 GeV and pseudorapidity $|\eta| < 2.4$. Moreover, a charged lepton veto is applied and the search strategy allows for a subleading jet activity provided it is well separated from the missing energy, the number of jets with $p_T > 30$ GeV, $|\eta| < 2.8$ and with an angular separation from the missing transverse momentum in azimuth $\Delta\phi$ of at least 0.4, being constrained to be at most 4. The selection is then divided into several exclusive and inclusive signal regions with different E_T^{miss} requirements. Whereas not directly targetting long-lived

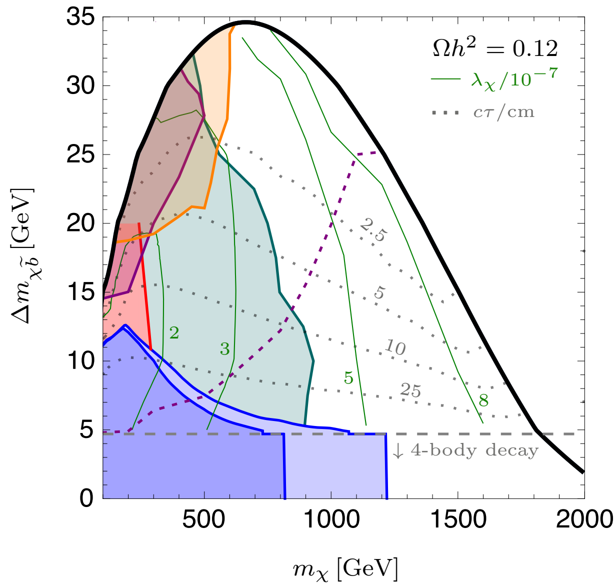

Figure 1: Allowed parameter space in the considered conversion-driven freeze-out scenario in the DM-mass vs. mass-splitting plane. The thin green and dotted grey curves denote contours of constant DM coupling and decay length, respectively (taken from [74]). We show 95% CL exclusion limits derived from the following analyses. The dark and light blue regions are excluded from R-hadron searches at the 8 [142] and 13 TeV LHC [143], respectively, as reinterpreted in [74]. The red and orange regions are excluded by the monojet [140] and multijet plus missing energy [141] analyses, respectively, while the teal and purple regions represent the limits obtained from the disappearing track [145] and displaced jet [146] searches, respectively. Finally, the purple dotted curve illustrates the limit that would be obtained after dropping the invariant mass cut of the last search (see the text for details).

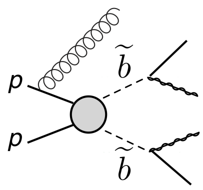

Figure 2: Production and decay diagram at LHC (in this case with ISR).

new physics, this search is able to constrain sbottom-neutralino configurations featuring a not too heavy neutralino $m_\chi \lesssim 300$ GeV for moderate mass splittings of about 10–20 GeV.

Here, we additionally update those bounds by including the impact of a recent ATLAS search for supersymmetry in a multijet plus missing energy final state [141]. As for the early Run 2 analysis, events exhibiting a large amount of missing energy ($E_T^{\mathrm{miss}} > 300$ GeV), a hard central leading jet ($p_T > 200$ GeV and $|\eta| < 2.8$), and no reconstructed electron or muon are preselected. However, in contrast, there is no limit on the number of subleading jets of $p_T > 50$ GeV, provided that the first three jets are well separated from the missing transverse momentum in azimuth ($\Delta\phi > 0.4$), and that the effective mass defined as the sum of the p_T of all reconstructed jets and the missing transverse energy satisfy $m_{\mathrm{eff}} > 800$ GeV. Different signal regions are then defined depending on the jet multiplicity and properties, the missing energy significance and the exact value of the effective mass. This analysis has been recast and validated within the MadAnalysis 5 framework [20, 71–73] with details of validation provided in the url [149], and the recast code available in [150].

We reinterpret this search, within the context of the simplified model described in this work. To this end, we generate Monte Carlo samples of 100000 parton-level events describing the production and decay of a pair of scalar bottom partners, possibly together with up to two additional QCD partons. Event generation is achieved with MadGraph5_aMC@NLO [19] and we use the MLM prescription to merge events featuring different jet multiplicities at the hard-scattering level [151]. Parton showering and hadronization are achieved with Pythia 8.2 [28] and event reconstruction is performed using the anti-k_T algorithm [152], as implemented in FastJet [153]. Detector simulation with parameters set to match the performance of the reinterpreted search has been performed with Delphes 3 [154]. The results of the reinterpretation are presented in Fig. 1, where the orange curve delineates the constraint on the parameter space in question, as an exclusion at 95 $\%$ using the CLs prescription. The constraint is dominated by the two jet bin with the lowest values of $m_{\rm eff}$ and missing transverse momentum criteria. This is understandable as we predominantly rely on radiation jets to pass the analysis selection, the new physics spectra being too compressed to lead to hard objects. The difference in the behaviour of the constrained region between the monojet analysis and the multijet plus missing energy analysis can be understood as stemming from two factors. The first one consists in the increased luminosity used in the multijet search. Secondly, the multijet search prioritizes larger mass gaps, while the monojet targets more compressed regions. Overall, we observe that up to $m_\chi \sim 500$ GeV is ruled for $\Delta m_{\tilde{\chi} b} \sim 35$ GeV.

Those typical searches for supersymmetry through the production of a large amount of missing energy in association with an important hadronic activity are however unsensitive to more compressed new physics spectra. In order to circumvert this issue, the CMS collaboration has performed a traditional search [155] for squarks and gluino using the M_{T2} kinematic variable [156] and extended it by including a signal region specifically focusing on events featuring a disappearing track that could be interpreted as the impact of a long-lived particle. In the standard search region, the selection vetoes the presence of leptons and either requires the presence of one central jet ($p_T > 30$ GeV and $|\eta| < 2.4$) or a low hadronic activity ($H_T < 1.2$ TeV) together with $E_T^{\rm miss} > 250$ GeV, or of a larger hadronic activity and $E_T^{\rm miss} > 30$ GeV. Once again, the missing transverse momentum is imposed to be well separated from the four leading jets, the missing transverse energy to be mainly originating from the jet activity and one finally requires $M_{T2} > 200$ GeV if $H_T < 1.5$ TeV, or $M_{T2} > 400$ GeV otherwise. The M_{T2} cut is lowered to 200 GeV in all cases if the event features a disappearing track. The implementation of such an analysis in the MadAnalyss 5 framework [20, 71–73] is ongoing.

3.2 Heavy stable charged particles

Towards large lifetimes, searches for heavy stable chareged particles become sensitive (see *e.g.* [138, 142–144]). These searches make use of observables related to large ionization energy loss and time of flight, typical for heavy charged particles traveling at low velocity through the detector. In this case, events are selected if they feature a well reconstructed track candidates with a large transverse momentum and a large amount of missing transverse momentum or a isolated muon candidate. In Fig. 1 we show the 95% CL exclusion from an reinterpretation of the 8 TeV [142] and early 13 TeV [143] CMS analysis for finite lifetimes performed in [74] as the dark and light blue curve (shaded area), respectively. The latter excludes the region of very small mass splittings $\Delta m_{\chi\tilde{b}} \lesssim 5$ GeV up to around 1.2 TeV. However, it quickly loses constraining power towards larger values of $\Delta m_{\chi\tilde{b}}$.

3.3 Disappearing tracks

Searches for disappearing tracks by the ATLAS [145] and CMS [137] collaborations also have the potential to constrain the scenario considered here, particularly for $\tilde{b}$ decay lengths in the range $c\tau \in [0.1 - 1]$ m. In the following, we analyze the sensitivity of the disappearing track ATLAS analysis using 36.1 fb^{-1} of 13 TeV LHC data [145]. We use the electroweak production event selection from the ATLAS analysis (despite our signal being produced via strong interactions), since the ATLAS strong production selection requires, besides the leading-p_T jet, several jets with a transverse momentum $p_T > 50$ GeV in the event. Such an option is usuaslly not featured by our signal, due to the small mass splitting $\Delta m_{\chi\tilde{b}}$ between the new physics states.

The kinematic event selection for electroweak production requires the presence of at least one jet with $p_T > 140$ GeV, a large amount of missing transvers energy ($E_T^{\rm miss} > 140$ GeV) that must be well separated in azimuth (with $\Delta\phi > 1$) from the four leading jets with $p_T > 50$ GeV. In addition, the selection vetoes the presence of reconstructed electron and muon, and events passing the kinematic selection so far are imposed to exhibit *tracklets* (short isolated tracks reconstructed solely from hits in the pixel detector, with no requirements from the SCT and TRT detectors [145]), with four specific properties. The corresponding requirements are:

1. *p_T and isolation*: The p_T of the candidate tracklet must be greater that 20 GeV, and the separation ΔR between the tracklet and any jet with $p_T > 50$ GeV must be greater than 0.4. Furthermore, the tracklet is required to be isolated (see [145] for details).
2. *Geometrical acceptance*: The tracklet properties must satisfy $0.1 < |\eta| < 1.9$.
3. *Quality requirements*: The tracklet is required to have hits in all four pixel layers (located at a radial distance $R \in [33.25,\ 122.5]$ mm from the interaction point).
4. *Disappearance condition*: The number of SCT hits associated with the tracklet must be zero.

The last two requirements may be satisfied if the $\tilde{b}$ decays outside the pixel detector and before the first SCT layer. Besides, the track hits on the first SCT layer from the jets coming out of the $\tilde{b}$ decay are required to have a minimal distance ($d_{\rm min}$) from the would-be hit of the extrapolated tracklet in this layer. This minimal distance is such that, taken the resolution $\sigma_{\rm SCT} \simeq 17$ μm of the SCT from [157], the χ^2 for matching the tracks is at least 15. That is,

$$d_{\rm min} > \sqrt{15}\,\sigma_{\rm SCT}\,. \tag{2}$$

Among the candidate tracklets (if more than one) passing all the above requirements, the one with the largest p_T is selected, and the analysis defines its signal region for tracklets with $p_T > 100$ GeV.

In order to estimate the sensitivity of this search to the present model, we generate $pp \to \tilde{b}\tilde{b}j$ (with $\tilde{b} \to \chi b$ decays) hard-scattering signal events with MADGRAPH5_AMC@NLO, imposing that the additional hard-jet satisfies $p_T > 140$ GeV[1] and the two $\tilde{b}$ states as yielding potential tracklets. We compute the fraction of events that pass the kinematic selection and the

[1]This allows for a preliminary estimate of the sensitivity. A full recasting of the ATLAS analysis including multipartonic matrix element merging, parton shower and hadronization is left for the future.

$\widetilde{b}$ tracklet selection at generator level. Furthermore, since $\widetilde{b}$ states form R-hadrons, we need to multiply the resulting efficiencies by the probability that the R-hadron ends up in a state with charge ± 1 (given approximately by 0.5, which we obtain from [138]). The *quality requirement* for the candidate tracklet is interpreted here as the $\widetilde{b}$ decaying outside the pixel detector volume (the ATLAS inner detector configuration measures are taken from Fig. 2 of [158]), and together with the tracklet *disappearance condition* ($\widetilde{b}$ decay before the first ATLAS SCT layer, together with its visible decay product satisfying the inequality (2)) mainly dictates the signal selection acceptance $\times$ efficiency. We also include in our analysis the efficiency for a generator level tracklet candidate to be identified as a tracklet at the reconstruction level, estimated approximately as 0.45 from the auxiliary material from [145].

The resulting excluded region is illustrated by the solid teal curve in Fig. 1, that shows that the analysis is sensitive to bottom partner masses ranging up to $m_{\widetilde{b}} \sim 900\,\text{GeV}$ and to splittings $\Delta m_{\chi\widetilde{b}} \sim 10\,\text{GeV}$ (corresponding to decay lengths $c\tau \sim 20\,\text{cm}$, in the "sweet-spot" of the ATLAS disappearing track search). Due to the high resolution of the ATLAS tracker, the condition (2) on the visible decay product does not have a significant effect even though the mass splitting here ($\mathcal{O}(10)$ GeV) is much larger than in the long-lived chargino model ($\mathcal{O}(100)$ MeV) targeted by the analysis. We expect this to also hold in a refined analysis performed at hadron level which is, however, left for future work.

3.4 Displaced jets

For decay lengths between a few millimeters and a few centimeters, the long-lived particle dominantly decays within the inner tracker, resulting in displaced b-jets and missing energy. A few ATLAS and CMS searches targeting this topology exist [146, 159, 160].

We consider here the ATLAS search for displaced vertices and missing energy using 32.8 fb^{-1} of 13 TeV LHC data [146]. This search is dedicated to final states exhibiting a large amount of missing energy and vertices containing at least five charged tracks displaced from the primary vertex by a distance between 4 mm and 30 cm. The benchmark scenario considered by the ATLAS analysis is a long-lived gluino simplified model, where the gluino decays into two jets and a neutralino. In this scenario, gluino masses of 1.5–2.5 TeV are excluded, the precise exclusion depending on the neutralino mass and gluino lifetime. The signal region considered by ATLAS requires the presence of a large amount of missing transverse energy ($E_T^{\text{miss}} > 250$ GeV), either one jet with $p_T > 70$ GeV or two jets with $p_T > 25$ GeV, and one or more displaced vertices containing at least 5 charged tracks and of invariant mass (m_{DV}) larger than 10 GeV.

Although the model considered here can produce events with large missing energy and sufficiently hard jets, the small mass gap between the long-lived parent and its daughter results in displaced vertices with invariant masses typically much smaller than 10 GeV. In Fig. 3, we compare the m_{DV} distribution for the gluino simplified model considered by ATLAS with masses $m_{\tilde{g}} = 625$ GeV and $m_{\tilde{\chi}_1^0} = 100$ GeV, and the model considered here with and without a large mass gap. For cases with a large mass gap, a sizeable fraction of the events contains vertices with large invariant masses. However, in the compressed case almost all events fail the $m_{\text{DV}} > 10$ GeV requirement.

In order to estimate the sensitivity of the search, we recast it by making use of the trigger and DV reconstruction efficiencies provided by ATLAS in the auxiliary material of Ref. [146]. We then use MadGraph5_aMC@NLO and Pythia 8.2 to generate hadron-level events and compute the signal efficiency for the model described in Sec. 2. Events are normalized to cross

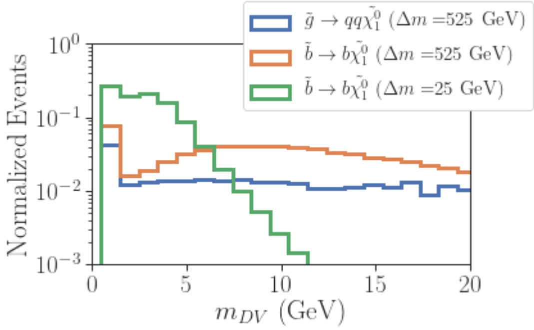

Figure 3: The invariant mass distribution for candidate displaced vertices. The blue histogram shows the distribution for a gluino simplified model with a large mass gap: $(m_{\tilde{g}}, m_{\tilde{\chi}_1^0}) = (625\text{ GeV}, 100\text{ GeV})$. The orange histogram shows the distribution for the model considered here with masses $(m_{\tilde{b}}, m_{\chi}) = (625\text{ GeV}, 100\text{ GeV})$, while the green histogram shows the same distribution but for the compressed scenario: $(m_{\tilde{b}}, m_{\chi}) = (625\text{ GeV}, 600\text{ GeV})$.

sections matching next-to-leading order calculations with the resummation of the next-to-next-to-leading threshold logarithms, as obtained from NNLL-FAST [161, 162].

As expected, most of the events fail the m_{DV} cut, suppressing the signal yield. The resulting 95% CL exclusion is illustrated by the solid purple curve in Fig. 1 that shows that only points with very large cross sections (small $\widetilde{b}$ masses) and a mass gap larger than 15 GeV are excluded. Since the main loss in sensitivity is due to the invariant mass requirement for the displaced vertices, we try to estimate what could be the reach resulting from relaxing this cut. In order to achieve this, we assume that the SM background remains unchanged and the DV reconstruction efficiency for vertices with $m_{\text{DV}} < 10\,\text{GeV}$ is the same as the one for $m_{\text{DV}} = 15\,\text{GeV}$. Although these certainly are optimistic assumptions, it allows us to use the efficiencies provided by the ATLAS collaboration when smaller mass cuts are used. The result is shown by the purple dashed line in Fig. 1, the excluded region being now significantly enhanced, extending up to 1 TeV bottom partner masses for small lifetimes (large mass splittings within the considered scenario).

Once again we stress that this is an optimistic and probably unrealistic projection. Nevertheless, it illustrates the impact of the invariant mass cut on the sensitivity to models with small mass gaps and reveals the potential gain of relaxing this cut. To achieve this, the background might be reduced by other means, *e.g.* by requiring a larger displacement. In fact, Fig. 1 shows a significant region where the displaced jets without a m_{DV} cut would outperform the disappearing track search (*e.g.* for $c\tau > 2.5\,\text{cm}$).

3.5 Delayed jets

Another option for distinguishing the long lifetime of some particles is to measure the timing information of their decay products, and search for delays with respect to the collision time. This method was exploited in a recent CMS analysis [147], where timing capabilities of the CMS electromagnetic calorimeter (ECAL) were used to identify non-prompt or "delayed" jets. The analysis is sensitive to long-lived particles decaying within the ECAL barrel volume extending up to 1.79 m and covering $|\eta| < 1.48$. The analysis uses only calorimetric information to reconstruct jets and imposes a set of quality criteria on the ECAL cells and energy fractions. Jet timing is calculated from the median of the times of ECAL cells associated with the jet, and is required to be at least 3 ns to discriminate from detector, beam, pileup and cosmic ray backgrounds. Events are imposed to have at least one delayed central jet with $p_T > 30$ GeV and $|\eta| < 1.48$. Additionally, one imposes that $E_T^{\rm miss} > 300$ GeV to eliminate SM multijet backgrounds and other beam-related backgrounds.

The analysis was interpreted using a gauge-mediated supersymmetry breaking model, where a 1–3 TeV long-lived gluino decays into a gluon and a 10 GeV gravitino. The large gluon-gravitino mass difference leads to high-p_T jets and a high signal efficiency. In the DM models considered here, the small $\widetilde{b}$-χ mass difference typically results in a much softer jet p_T spectrum. However, a preliminary study of events generated with MADGRAPH5_AMC@NLO (hard-scattering), PYTHIA 8.2 (parton showering and hadronization) and DELPHES 3 (detector simulation) leads to a sizable fraction of events passing the jet p_T and $E_T^{\rm miss}$ selection, especially for points with a relatively high mass difference. The larger cross sections for lower masses would further improve the signal significance in this very low background analysis. Where the simulation of delayed jet selection criteria is non-trivial in existing public tools, delayed jet selection efficiencies depending on the jet transverse momentum and pseudorapidity would be a fundamental requirement for obtaining reliable estimates of the sensitivity of this analysis.

4 Conclusions

In this contribution, we considered a conversion-driven feeze-out DM scenario predicting long-lived particles with decay length $\mathcal{O}(1\,\text{mm} - 1\,\text{m})$ at the LHC. The scenario is characterized by small DM couplings and relatively small mass splittings ($\mathcal{O}(10)$ GeV) in the dark sector, *i.e.* between the parent particle pair-produced at the LHC and the DM particle it decays into. We considered searches for heavy stable charged particles (R-hadrons), disappearing tracks, displaced (and delayed) jets as well as prompt missing energy searches covering the whole range of possible decay lengths. The strongest constraint can be reached towards the upper edge of the occurring decay lengths within the model, $c\tau \sim 1\,\text{m}$, by searches for heavy stable charged particles, reaching DM masses around 1.2 TeV. For intermediate lifetimes, searches for disappearing tracks are most sensitive and constrain DM masses up to ~ 900 GeV for $\Delta m_{\chi\widetilde{b}} \sim$ 10 GeV (which corresponds to a decay length of around 20 cm). Towards smaller lifetimes the search loses sensitivity. Finally, for $c\tau \lesssim 2.5\,\text{cm}$ ($\Delta m_{\chi\widetilde{b}} \gtrsim 25\,\text{GeV}$), the considered multijet plus missing energy search the most sensitive, constraining DM masses ranging up to around 600 GeV.

The search for displaced jets is only sensitive to a very small region of the parameter space, with masses below $m_\chi = 500$ GeV – a region being already excluded by the disappearing tracks and missing energy search. This is mainly due to the lower invariant mass cut on the tracks arising from the displaced vertex which is affordable in the scenario considered in the experimental analysis with a large mass gap, but that rejects most of the signal for the considered model with small mass splittings. Relaxing this cut potentially has a very large effect and would render the displaced jet search to be the most sensitive for $\Delta m_{\chi\widetilde{b}} \gtrsim 15$ GeV ($c\tau \lesssim 10$ cm). Determining whether this is possible (above a certain minimal displacement) requires further studies considering the relevant backgrounds.

Acknowledgements

We thank G. Bélanger, A. Bharucha, B. Bhattacherjee, N. Desai, A. Goudelis, P. Pani and H.-S. Shao for fruitful discussions. J.H. acknowledges support from the F.R.S.-FNRS, of which he is a postdoctoral researcher. The work of A.L. was supported by the São Paulo Research Foundation (FAPESP), under the project 2015/20570-1. J.M.N. acknowledges support from the Ramón y Cajal Fellowship contract RYC-2017-22986, from the Spanish MINECO's "Centro de Excelencia Severo Ochoa" programme under grant SEV-2016-0597, from the European Union's Horizon 2020 research and innovation programme under the Marie Sklodowska-Curie grant agreements 690575 (RISE InvisiblesPlus) and 674896 (ITN ELUSIVES) as well as from the Spanish Proyectos de I+D de Generación de Conocimiento via the grant PGC2018-096646-A-I00.